ORIGINAL ARTICLE

Full title:

Spinal nerve defects in mouse embryos prenatally exposed to valproic acid

Short running title:

Spinal nerve defects by prenatal VPA

Authors:

Juramt Bold • Hiromi Sakata-Haga[*] • Yoshihiro Fukui

Affiliation

Department of Anatomy and Developmental Neurobiology, Institute of Biomedical Sciences, Tokushima University Graduate School, Tokushima 770-8503, Japan

Correspondence: Hiromi Sakata-Haga[*], Ph D

[*]Present address: Department of Anatomy, Kanazawa Medical University, 1-1 Daigaku, Uchinada, Ishikawa 920-0293, Japan. Tel.: +81-76-218-8113 Fax: +81-88-218-8189.

Email: h-sakata@kanazawa-med.ac.jp

Abstract

To examine in detail spinal nerve defects induced by prenatal exposure to valproic acid in mice, pregnant ICR mice were subcutaneously injected with a single dose of 400 mg/kg valproic acid on gestational day 6, 7, 8, or 9, and their embryos were observed on gestational day 10. The whole-mount immunostaining using an anti-neurofilament antibody allowed us to identify spinal nerve defects, such as a loss of bundle, anastomosis among bundles arising from adjacent segment, and a disrupted segmental pattern of the dorsal root ganglia, in valproic acid-exposed embryos. The prevalence of spinal nerve defects was the highest in the embryos exposed to valproic acid on gestational day 8 among the experimental groups. Then, effects of the administration dose of valproic acid on the prevalence of spinal nerve defects were examined on gestational day 10 and found to be dose-dependently increased. It was noteworthy that all embryos exposed to 600 mg/kg of valproic acid on gestational day 8 suffered spinal nerve defects. Folic acid (3 mg/kg/day) supplementation during gestational day 6 to10 suppressed the prevalence of valproic acid-induced neural tube defects, which are common malformations in offspring prenatally exposed to valproic acid, but not that of spinal nerve defects. Thus, the spinal nerve defects due to prenatal valproic acid exposure might be induced by mechanisms different from those of neural tube defects. Because spinal nerve defects were predicted to be caused by the disrupted segmental arrangement of the somites and/or that of neural crest cells which was the origin of the dorsal root ganglia and/or abnormal polarity of the somite, this mouse model with spinal nerve defects at high incidence, would be useful to examine the effects of valproic acid on somitogenesis and morphogenesis of somite-associated structures.

Keywords

Folic acid · Developmental neurotoxicity · Mice · Spinal nerve ·

Valproic acid

Introduction

Valproic acid (VPA) has been commonly used for treatment of epilepsy, and has also been recognized as a teratogen. Single use of VPA during pregnancy may possibly increase the risk of spina-bifida, polydactyly, clubfoot, cleft palate, ventricular septal defect, atrial septal defect, and hypospadias, in human (review in Jentink et al., 2010). Although it has been recommended to withdraw VPA during pregnancy, it still cannot be discontinued in a subset of epileptic women in order to have good seizure control, which is common to them even during pregnancy (Ornoy, 2006).

Details of VPA teratogenicity have been confirmed in studies using animal models of various species, including, mouse, rat, chick, zebrafish, and also monkey (reviewed in Ornoy, 2009). Previous reports demonstrated that prenatal VPA exposure may possibly induce developmental dismorphology, such as exencephaly, skeletal malformations, and cardiac defects (Padmanabhan and Hameed, 1994). Prenatal VPA exposure also has been suspected to disturb behavioral development, even in the absence of malformation (Meador et al., 2013). Epidemiological studies showed that VPA exposure *in utero* increased the incidence of autism and autism spectrum disorder in human (Bromely et al., 2008; Christensen et al., 2013), and prenatal VPA-exposed animals have been interesting models of autism these days (Bambini-Junior et al., 2011; Narita et al., 2010; Roullet et al., 2010).

Menegola and her colleagues reported morphological defects of spinal nerves (spinal nerve defects; SNDs) in rat embryos exposed to VPA *in utero* (Menegola et al., 1999). It was also well known that VPA exposure *in utero* induced axial skeletal malformations, such as fusion of the adjacent vertebrae (Okada et al., 2004;

Padmanabhan and Hameed, 1994). Because the vertebrae are derived from the sclerotomes, which differentiated from the somites, it has been suspected that the vertebral malformation seen in VPA-exposed offspring could be caused by disruption of somitogenesis (Di Renzo et al., 2010; Menegola et al., 1999). As well as generation of the vertebrae, segmental fascicle formation of the spinal nerves is closely associated in the somites, although spinal nerves do not arise from the somites, unlike the vertebrae. Thus, it was predictable that the disrupted somite formation in VPA-exposed offspring might consequently induce also SNDs.

The somites are generated by periodic segmentation of the paraxial mesoderm with a fine process regulated by several molecular systems to control the number of each somite and timing of their formation, size, orientation and axial identity (see Gilbert, 2014). The “Clock and wavefront model” is one of the well-known mechanisms to explain the fine controlled process (Baker et al., 2006; Cooke and Zeeman, 1976; Dequéant and Pourquîé, 2008). Somite polarity also contributes to braid striking segmental arrangement of the spinal nerves. In addition, the metameric arrangement of the dorsal root ganglia, that derived from the subset of neural crest cells and arise sensory axons, is partially caused by segmental settlement of migrated neural crest cells. Although only a few studies examined the effects of VPA on somitogenesis-related molecules (Barnes et al., 1996; Di Renzo et al., 2010), it has never been examined about the effects of VPA on the somite clock system, the repulsive mechanism for segmental arrangement of spinal nerve axons, and segmental migration of neural crest cells.

Although VPA-induced SNDs were observed in rats, but still not yet in mice and zebrafish, which are commonly used to examine the mechanism of somite formation (see reviews, Hubaud and Pourquie, 2014; Yabe and Takada, 2016). In addition, the

morphological phenotype of prenatal VPA-exposed offspring was different between rat and mouse. For example, whereas exencephaly, which is a type of NTDs in the anterior part of the neural tube, has been frequently observed in mice after prenatal VPA exposure, it was not common in VPA-exposed rats. Thus, the prenatal VPA-exposed mouse model, in which both NTDs and SNDs can be induced at a high incidence, could well serve to identify the mechanisms of dismorphology induced by VPA. The aim of the present study was the detection of SNDs in prenatally VPA-exposed mouse embryos and examination of developmental stage-dependent and dose-dependent changes of the prevalence of the SNDs induced by VPA.

Materials and methods

Pregnant ICR mice were obtained from Japan SLC (Hamamatsu, Japan). The day of presence of a vaginal plug was referred to as gestational day (GD) 0. All mice used for the present study were maintained in a temperature-controlled room (23 ±1°C) under a 12-hour/12-hour of light and dark cycle and allowed free access to lab chow (MF, Oriental Yeast Co., Tokyo, Japan) and tap water. All animal procedures were conducted according to the Guide for the Care and Use of Laboratory Animals, and were reviewed by the Institutional Animal Care and Use Committee of the University of Tokushima. Great care was taken to minimize the number of animals used, and their suffering.

As Experiment #1, a single dose of 400 mg/kg VPA was subcutaneously injected to pregnant ICR mice on GD 6, 7, 8, or 9. VPA (sodium valproic acid, Sigma-Aldrich, MO) was dissolved into saline. As controls for each VPA-exposed group, pregnant mice received saline administration on the same schedule. In Experiment #2, pregnant mice

received subcutaneously VPA administration on GD 8 as a dose of 100, 200, 400, or 600 mg/kg in order to examine a dose-related effect of prenatal VPA exposure on the spinal nerve development. In Experiment #3, pregnant mice that received 400 mg/kg VPA on GD 8 were orally administered folic acid (Sigma-Aldrich, MO) at a dose3 mg/kg/day or vehicle (distilled water) during GD 6 to 10.

On GD 10, pregnant mice were dissected under deep anesthesia, their embryos were removed and immersed in 4% paraformaldehyde/0.1 M phosphate buffer (4% PFA, pH 7.2) and fixed overnight in 4% PFA. After washing with PBS, the embryos were immersed in 6% H_2O_2 in methanol for 60-min at room temperature and stored in methanol at -30℃ until use. The procedure previously described (Lee et al, 1995) was modified for the whole mount immunostaining in the present study. Briefly, embryos were incubated for three days in an anti-neurofilament antibody (2H3, 1:300, Developmental Studies Hybridoma Bank, IA), at 4°C. Next, the embryos were incubated with horseradish peroxidase-conjugated anti-mouse IgG antibody (1:200, MBL, Nagoya, Japan) overnight at 4°C. The immunoreactivity was then visualized with an ice cold Tris buffer/0.1% Triton X-100 containing 2.5 μg/ml 3,3-diaminobenzidine tetrahydrochloride (Nakarai, Kyoto, Japan) under the presence of 0.003% H_2O_2. Immunostained embryos were binocularly observed (Leica, Wetzlar, Germany) and images were obtained by an imaging system (DS-L3, Nikon, Tokyo, Japan). Sometimes embryos were artificially ruptured during sampling or staining procedure, resulting in unclear staining in the whole mount immunostaining, or showed severe developmental delay beyond recognition of SNDs and/or NTDs. In these cases, the embryos were eliminated from calculation of the prevalence of SNDs or NDTs. The numbers of litters and embryos using each observation were listed in Table 1.

Statistical analyses were conducted using a software, Statcel 3 (OMS, Tokorozawa, Japan). Fisher's exact probability test was applied to compare the prevalence of SNDs or NTDs between a VPA-exposed group and its control. Effects of FA supplementation on the prevalence of SNDs or NTDs were evaluated by χ^2 test. Statistical significance was considered at $p < 0.05$.

Results

As previously described (Osumi et al., 1997), the whole-mount immunostaining using an anti-neurofilament antibody clearly detected fiber bundles and dorsal root ganglia consisting of the spinal nerves and also fiber bundles of the several cranial nerves and their ganglia (Fig. 1). VPA-exposed mice showed a diverse type of SNDs, such as loss of nerve bundle with or without disrupted segmental arrangement of the spinal ganglia (Fig. 2B and C, respectively), an anastomosis among bundles arise from adjacent segment, (Fig. 2D). Excencephaly, which is a commonly reported NTD in mice after prenatal VPA exposure, was also observed in our VPA-exposed mouse embryos (Fig. 2E).

In Experiment #1, we examined developmental stage-related change of prevalence of SNDs and NTDs induced by VPA. The highest prevalence of SNDs was marked in the embryos derived from dams administered VPA on GD 8 (Fig. 3 A). Statistical analysis revealed a significant difference in prevalence between mouse embryos exposed to VPA on GD 8 and their control group ($p<0.01$). Prevalence of NTDs was significantly higher in the embryos exposed to VPA on GD 7 or GD8 compared to each control group ($p<0.01$).

In Experiment #2, a dose-related change in the prevalence of SNDs was examined using embryo exposed to VPA on GD 8, which is the day showing the highest prevalence of SNDs induced by VPA in Experiment #1. Dose-dependent administration increase in prevalence was confirmed in both SNDs and NTDs, although it was more noticeable in SNDs. 100 mg/kg VPA administration on GD 8 was not sufficient to induce SNDs ($p=0.48$) (see Fig.4).

Preventive effects of folic acid supplementation were examined in Experiment #3 (Fig. 5). As previously reported, folic acid supplementation suppressed the incidence of NTDs. On the other hand, prevalence of SNDs induced by VPA was not altered by folic acid supplementation.

Discussion

In the present study, we showed various types of SNDs in mouse models of prenatal VPA exposure. The most sensitive period of VPA exposure to induce the SNDs was GD 8 in mice. The prevalence of SNDs was VPA dose-dependently increased by administration on GD 8, and it was notable that all of the embryos exposed to VPA on GD 8 at a dose of 600 mg/kg suffered SNDs, although only about 32% of embryos in the same group showed NTDs. Folic acid supplementation during GD 6 to GD 10 was effective to suppress the prevalence of NTDs but not that of SNDs caused by prenatal VPA exposure. Thus, the mechanism of SNDs by prenatal VPA exposure might be different from that of NTDs.

The striking segmental fascicle formation of the spinal nerve is closely associated with the somite. Especially, somite polarity contributes to braid segmental arrangement

of the spinal nerves. During the development, both sensory and motor axons, that sprouting from the dorsal root ganglia and ventral part of the neural tube, respectively, are confined to the anterior half of the each segmented sclerotome, resulting from rejection by its posterior half (Kuan et al., 2014). In addition, the metameric arrangement of the dorsal ganglia that derived from the subset of neural crest cells and arise sensory axons, is also contributed by segmental migration system of neural crest cells. A number of candidate molecules, such as ephrin-B1 that is expressed in the posterior halves of the sclerotome and also controls fasciculation of axons, neuropilin 1 that is required for segmental arrangement of the dorsal ganglion, neuropilin 2 that is required for segmental migration of neural crest cells, and semaphorin 3A that is expressed in the posterior halves of the sclerotome, for this restricted distribution of spinal nerve axons were reported (Luxey et al., 2013; Roffers-Agarwal and Gammill, 2009; Vermeren et al., 2000). Neural crest cells also contribute to generation of somite polarity, due to their restricted migration into the anterior half of each somite. The effects of VPA on the repulsive mechanism for segmental arrangement of spinal nerve axons and segmental migration of neural crest cells have never been examined. However, it was reported that VPA affected migration and proliferation of neural crest cells (Fuller et al., 2002) and inhibited the differentiation of branchial ganglia, especially in the dorsal part of them, deriving from neural crest cells (Gofflot et al, 1996). Thus, it is necessary to investigate an involvement of neural crest cells in VPA-induced SNDs in further experiments.

The SNDs induced by prenatal VPA exposure are likely to be caused by odd arrangement of the somites, because it was previously reported that prenatal VPA exposure disrupted striking segmental arrangement of somites (Di Renzo et al., 2010). It

was suspected that the disrupted segmental arrangement of somites might have contributed to dismorphogenesis of vertebrates and also SNDs after prenatal VPA exposure. Even so, it has been never examined yet how VPA affects somitogenesis. Somitogenesis is accomplished with several components, such as separation of the somite, periodicity, epithelialization, specification, and differentiation, and a number of molecules are identified as key agents contributing to this dynamic process (see Gilbert, 2014). For example, Notch signaling pathway plays an important role to determine where somite boundaries are formed and Lunatic fringe, a modulator of the Notch receptor and is expressed in the region of the presumptive boundary in presomitic mesoderm, contributes to establish a morphological boundary between each somite (Sato et al., 2002). Interestingly, the *lunatic fringe* mutant mice showed fusion of adjacent vertebrae and disruption of the periodic pattern of the dorsal root ganglia (Evrard et al., 1998), resembling with prenatally VPA-exposed mice. Because it has been reported that VPA modulated Notch signaling (Stockhausen et al., 2005; Sun et al., 2015), a disruption of Notch signaling is suspected of relating to VPA-induced SNDs. However, it remains unclear whether the cause of SNDs was only the disrupted metameric arrangement of somite and/or other factors, such as somite polarity and migration of neural crest. Thus, it was expected that mechanisms of VPA-induced morphological defects would become evident in further experiments using this VPA-exposed mice model showing a high incidence of SNDs.

Conflict of interest The authors declare no conflicts of interest in this work.

Acknowledgement

This work was supported by JSPS KAKENHI Grant Number 23591595 and 26461634.

References

Baker RE, Schnell S, Maini PK (2006) A clock and wavefront mechanism for somite formation. Dev Biol 293:116-126.

Bambini-Junior V, Rodrigues L, Behr GA, Moreira JC, Riesgo R, Gottfried C (2011) Animal model of autism induced by prenatal exposure to valproate: behavioral changes and liver parameters. Brain Res 1408:8-16.

Barnes GL Jr, Mariani BD, Tuan RS (1996) Valproic acid-induced somite teratogenesis in the chick embryo: relationship with Pax-1 gene expression. Teratology 54:93-102.

Bromely RL, Mawer G, Clayton-Smith J, Baker GA (2008) Autism spectrum disorders following in utero exposure to antiepileptic drugs. Neurology 71:1923-1924.

Cooke K, Zeeman EC (1976) A clock and wavefront model for control of the number of repeated structures during animal morphogenesis. J Theor Biol 58:455-476.

Christensen J, Grønborg TK, Sørensen MJ et al. (2013) Prenatal valproate exposure and risk of autism spectrum disorders and childhood autism. JAMA 309:1696-1703.

Dequéant ML, Pourquié O (2008) Segmental patterning of the vertebrate embryonic axis. Nat Rev Genet 9:370-382.

Di Renzo F, Broccia ML, Giavini E, Menegola E (2010) VPA-related axial skeletal defects and apoptosis: a proposed event cascade. Reprod Toxicol 29:106-111.

Evrard YA, Lun Y, Aulehla A, Gan L, Johnson RL (1998) *lunatic fringe* is an essential

mediator of somite segmentation and patterning. Nature 394:377-381.

Fuller LC, Cornelius SK, Murphy CW, Wiens DJ (2002) Neural crest cell motility in valproic acid. Reprod Toxicol 16:825-839.

Gilbert SF (2014) Developmental biology (Tenth edition). Sinauer Associates, Sunderland.

Gofflot F, van Maele-Fabry G, Picard JJ (1996) Cranial nerves and ganglia are altered after in vitro treatment of mouse embryos with valproic acid (VPA) and 4-en-VPA. Brain Res Dev Brain Res 93:62-69.

Hubaud A, Pourquié O (2014) Signalling dynamics in vertebrate segmentation. Nat Rev Mol Cell Biol 15:709-721.

Jentink J, Loane MA, Dolk H et al. (2010) Valproic acid monotherapy in pregnancy and major congenital malformations. N Engl J Med 362:2185-2193.

Kuan C-Y K, Tannahill D, Cook GMW, Keynes RJ (2004) Somite polarity and segmental patterning of the peripheral nervous system. Mechan Dev 121: 1055-1068.

Lee YM, Osumi-Yamashita N, Ninomiya Y, Moon CK, Eriksson U, Eto K (1995) Retinoic acid stage-dependently alters the migration pattern and identity of hindbrain neural crest cells. Development 121:825-837.

Luxey M, Jungas T, Laussu J, Audouard C, Garces A, Davy A (2013) Eph: ephrin-B1 forward signaling controls fasciculation of sensory and motor axons. Dev Biol 383: 264-274.

Meador KJ, Baker GA, Browning N et al. (2013) Fetal antiepileptic drug exposure and cognitive outcomes at age 6 years: a prospective observational study. Lancet Neurol 12:244-252.

Menegola E, Broccia ML, Prati M, Giavini E (1999) Morphological alterations induced

by sodium valproate on somites and spinal nerves in rat embryos. Teratology 59:110-119.

Narita M, Oyabu A, Imura Y et al. (2010) Nonexploratory movement and behavioral alterations in a thalidomide or valproic acid-induced autism model rat. Neurosci Res 66:2-6.

Okada A, Kurihara H, Aoki Y, Bialer M, Fujiwara M (2004) Amidic modification of valproic acid reduces skeletal teratogenicity in mice. Birth Def Res 71:47-53.

Ornoy A (2006) Neuroteratogens in man: an overview with special emphasis on the teratogenicity of antiepileptic drugs in pregnancy. Reprod Toxicol 22:214-226.

Ornoy A (2009) Valproic acid in pregnancy: How much are we endangering the embryo and fetus? Reprod Toxicol 28:1-10.

Osumi N, Hirota A, Ohuchi H et al. (1997) *Pax-6* is involved in the specification of hindbrain motor neuron subtype. Development 124:2961-2972.

Padmanabhan R, Hameed MS (1994) Exencephaly and axial skeletal malformations induced by maternal administration of sodium valproate in the MF1 mouse. J Craniofac Genet Dev Biol 14:192-205.

Roffers-Agarwal J, Gammill LS (2009) Neuropilin receptors guide distinct phases of sensory and motor neuronal segmentation. Development 136: 1879-1888.

Roullet FI, Wollaston L, DeCatanzaro D, Foster JA (2010) Behavioral and molecular changes in the mouse in response to prenatal exposure to the anti-epileptic drug valproic acid. Neuroscience 170:514-522.

Sato Y, Yasuda K, Takahashi Y (2002) Morphological boundary forms by a novel inductive event mediated by Lunatic fringe and Notch during somatic segmentation. Development 129:3633-3644.

Stockhausen MT, Sjölund J, Manetopoulos C, Axelson H (2005) Effects of the histone deacetylase inhibitor valproic acid on Notch signalling in human neuroblastoma cells. Br J Cancer 92:751-759.

Sun G, Mackey LV, Coy DH, Yu CY, Sun L (2015) The histone deacetylase inhibitor valproic acid induces cell growth arrest in hepatocellular carcinoma cells via suppressing Notch signaling. J Cancer 6:996-1004.

Vermeren MM, Cook GMW, Johnson AR, Keynes RJ, Tannahill D (2000) Spinal nerve segmentation in the chick embryo: Analysis of distinct axon-repulsive systems. Dev Biol 225:241-252.

Yabe T, Takada S (2016) Molecular mechanism for cyclic generation of somites: lessons from mice and zebrafish. Develop Growth Differ 58:31-42.

Fig. 1 Whole mount immunostaining using anti-neurofilament antibody in mouse embryo on GD 10. ***tel*** telencephalon, **ov** opitic vesicle, ***he*** heart, ***ab*** anterior limb bud, ***pb*** posterior limb bud, **III** oculomotor nerve, **V(G)** trigeminal ganglion, $\mathbf{V_1}$ ophthalmic nerve, $\mathbf{V_2}$ maxillary nerve, $\mathbf{V_3}$ mandibular nerve, **VII** facial nerve, **X** vagus nerve, **XII** hypoglossal nerve, **C1~8**, cervical nerves, **Th 1~13** thoracic nerves, **L 1~5** lumbar nerves. Scale bar = 1 mm.

Fig. 2 SNDs and excencephaly seen in prenatal VPA-exposed mouse embryo on GD 10. Whole mount-immunostained intact embryo (A) and VPA-exposed embryos (B, C, D, and E), with high magnification of the rectangle framed region on each (A', B', C', D', and E', respectively). The intact embryo showed striking arrangement of fascicle and dorsal ganglia of the spinal nerves (A and A'). VPA-exposed mouse embryos showed various types of SNDs, such as loss of fiber bundle (arrows) with (B and B') or without (C and C') disruption of segmentation of the dorsal root ganglia (an asterisk in B'), an anastomosis among bundles which arose from adjacent segments (D and D', arrowheads) E, a prenatal VPA-exposed embryo with excencephaly.

Fig. 3 VPA (400 mg/kg) exposure stage-related difference in prevalence of SNDs (A) and NTDs (B) in mice. Only the embryos exposed to VPA on GD 8 showed significant increase in prevalence of SNDs. Significant increase in prevalence of NTDs was detected in the embryos exposed to VPA on either GD 7 or GD 8. * $p<0.01$ v.s. each saline-administered control group.

Fig. 4 VPA dose-related differences in incidence of SNDs (A) and NTDs (B) in mice exposed to VPA on GD 8. Prevalence of both SNDs and NTDs by VPA was increased in an administration dose-dependent manner, whereas that in SNDs was more prominent. * $p<0.05$, ** $p<0.01$ v.s. a saline-administered control group.

Fig. 5 Preventive effect of folic acid supplementation on prenatal VPA-induced SNDs and NTDs. Folic acid supplementation suppressed incidence of NTDs, but not that of SNDs. * $p<0.05$ v.s. a DW and VPA-administeredS control group.

Table 1 Number of litters and embryos

	Litter	Total embryos	Observation of SNDs	Observation of NTDs
Intact	4	38	55	51
<Experiment #1>				
Sal GD6	4	51	51	49
VPA GD6	3	42	41	40
Sal GD7	2	23	23	20
VPA GD7	7	91	87	82
Sal GD8	4	54	54	48
VPA GD8	7	88	83	80
Sal GD9	3	38	35	33
VPA GD9	3	36	35	31
<Experiment #2>				
Sal	4	54	54	48
VPA 100	4	63	63	45
VPA 200	2	32	29	28
VPA 400	7	88	83	80
VPA 600	2	28	28	22
<Experiment #3>				
DW/VPA 400	8	124	122	103
FA/VPA 400	8	108	107	89

Fig. 1

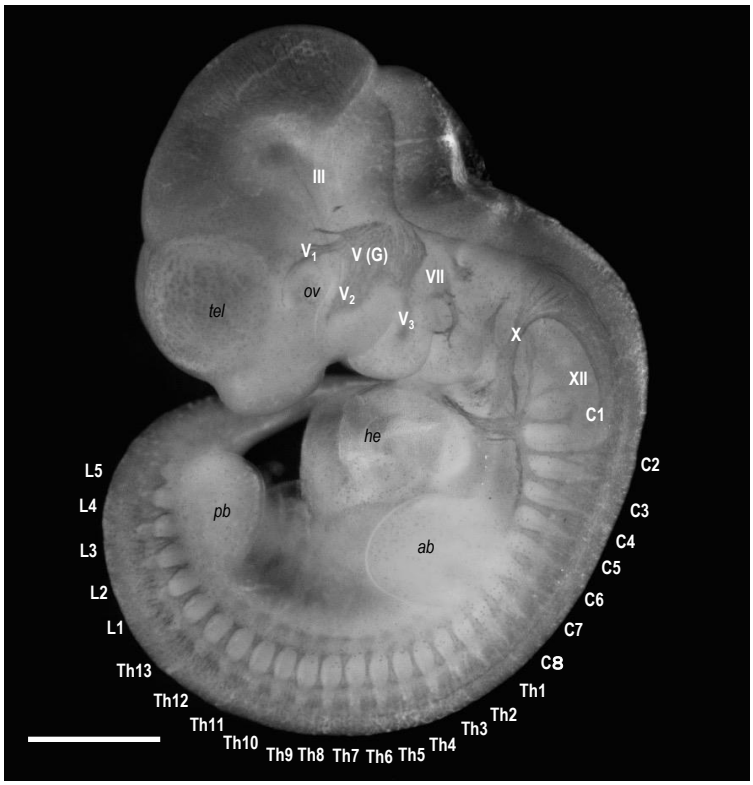
III
V1
V (G)
VII
ov
V2
tel
V3
X
XII
C1
he
C2
L5
L4
pb
C3
ab
C4
L3
C5
L2
C6
L1
C7
C8
Th13
Th1
Th12
Th2
Th11
Th3
Th10
Th4
Th9 Th8 Th7 Th6 Th5

Fig. 2

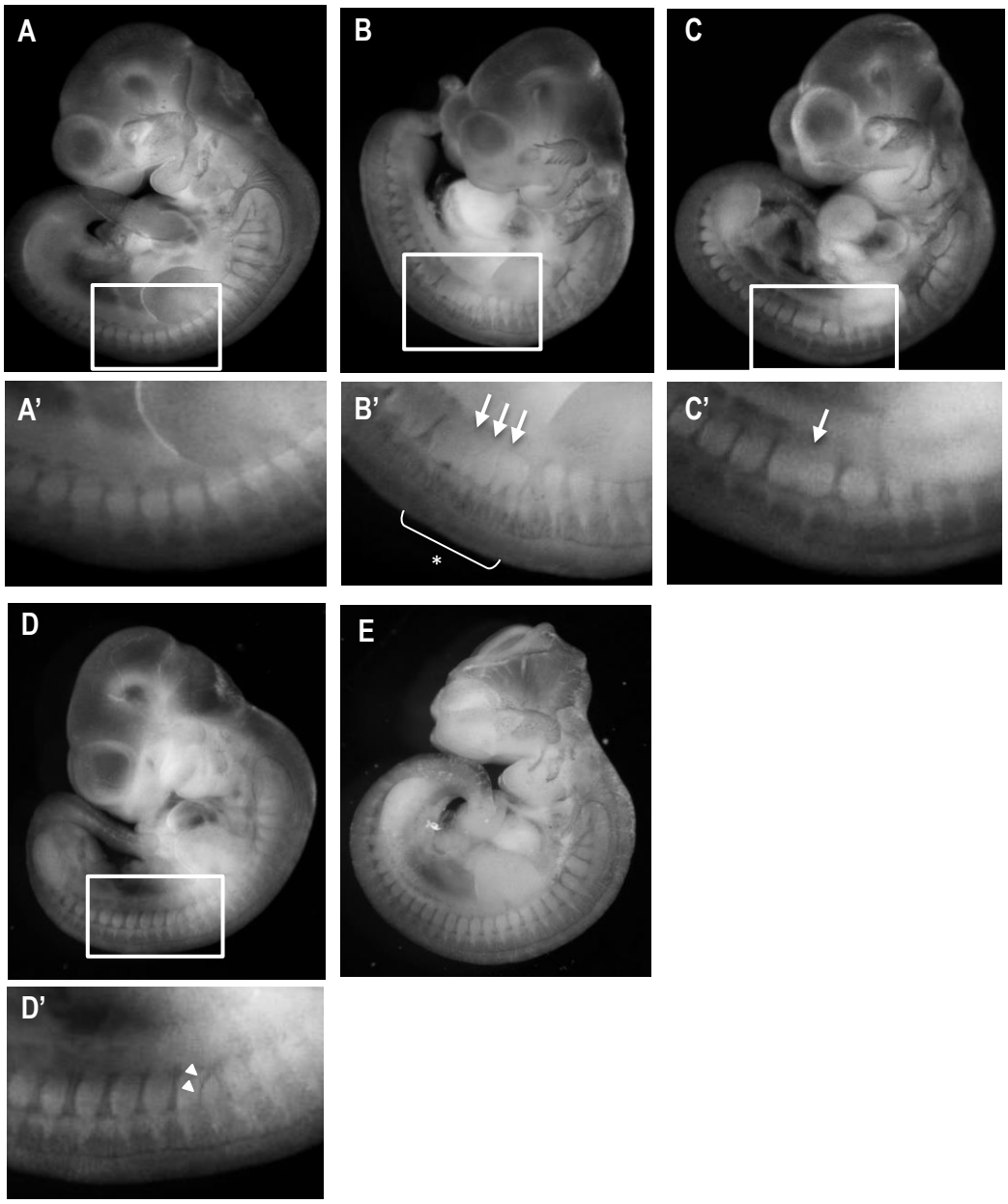

Fig. 3

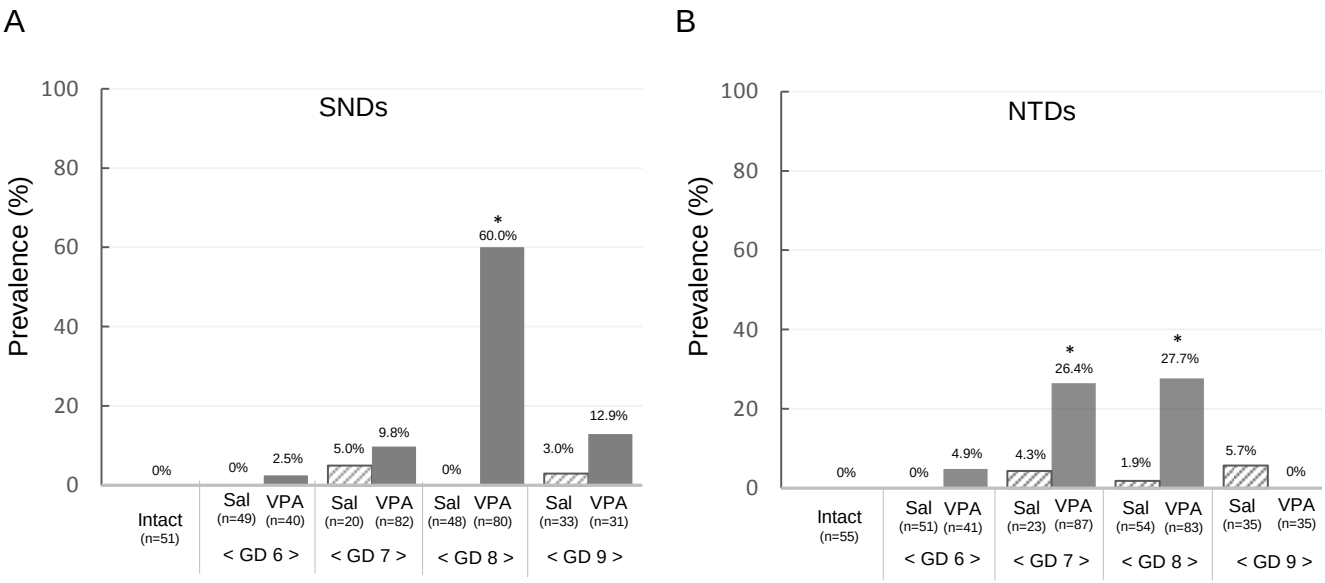
A
SNDs
Prevalence (%)
100
80
60
40
20
0
0%
0%
2.5%
5.0%
9.8%
0%
*
60.0%
3.0%
12.9%
Intact (n=51)
Sal (n=49)
VPA (n=40)
Sal (n=20)
VPA (n=82)
Sal (n=48)
VPA (n=80)
Sal (n=33)
VPA (n=31)
< GD 6 >
< GD 7 >
< GD 8 >
< GD 9 >
B
NTDs
Prevalence (%)
100
80
60
40
20
0
0%
0%
4.9%
4.3%
*
26.4%
1.9%
*
27.7%
5.7%
0%
Intact (n=55)
Sal (n=51)
VPA (n=41)
Sal (n=23)
VPA (n=87)
Sal (n=54)
VPA (n=83)
Sal (n=35)
VPA (n=35)
< GD 6 >
< GD 7 >
< GD 8 >
< GD 9 >

Fig. 4

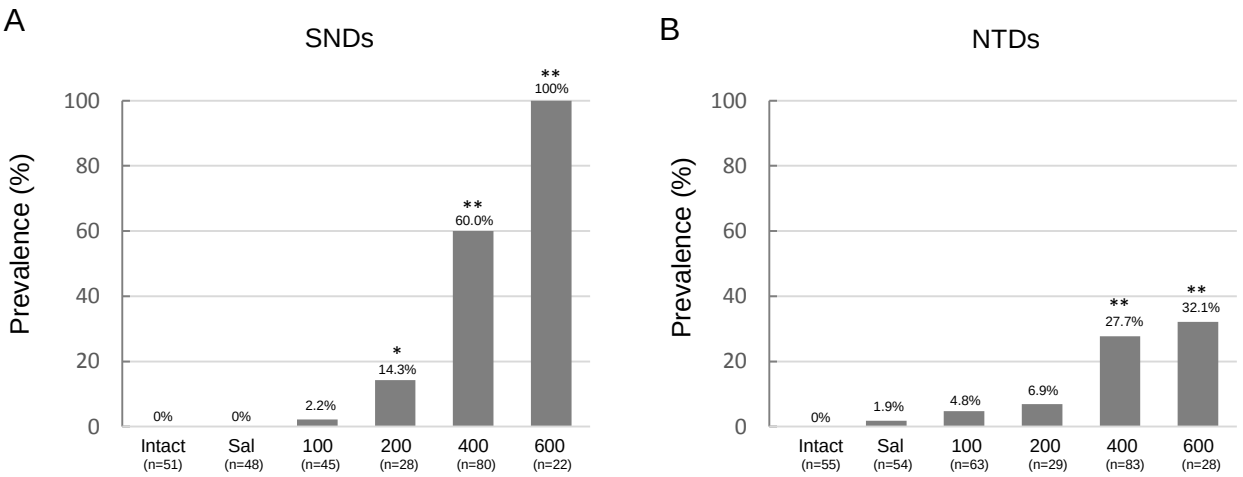
A
SNDs
Prevalence (%)
100
80
60
40
20
0
0%
0%
2.2%
*
14.3%
**
60.0%
**
100%
Intact (n=51)
Sal (n=48)
100 (n=45)
200 (n=28)
400 (n=80)
600 (n=22)
B
NTDs
Prevalence (%)
100
80
60
40
20
0
0%
1.9%
4.8%
6.9%
**
27.7%
**
32.1%
Intact (n=55)
Sal (n=54)
100 (n=63)
200 (n=29)
400 (n=83)
600 (n=28)

Fig. 5

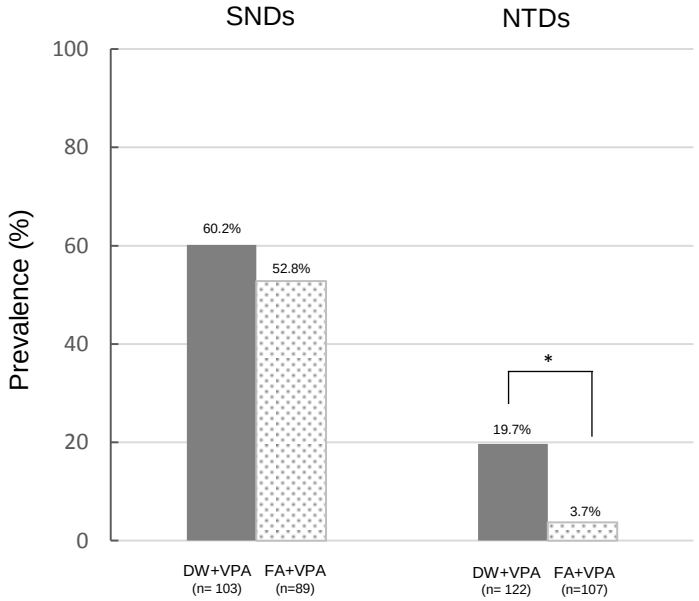
SNDs
NTDs
100
80
60
40
20
0
Prevalence (%)
60.2%
52.8%
19.7%
3.7%
*
DW+VPA
(n= 103)
FA+VPA
(n=89)
DW+VPA
(n= 122)
FA+VPA
(n=107)

*